

Three mixed ligand mononuclear Zn(II) complexes of 4-acyl pyrazolones: Synthesis, characterization, crystal study and anti-malarial activity

Irfan Shaikh^a, R.N. Jadeja^{a,*}, Rajesh Patel^b

^a Department of Chemistry, Faculty of Science, The Maharaja Sayajirao University of Baroda, Vadodra 390 002, India

^b Department of Bioscience, Veer Narmad South Gujarat University, Surat 395007, India

ARTICLE INFO

Article history:

Received 20 February 2020

Accepted 18 March 2020

Available online 23 March 2020

Keywords:

Acyl pyrazolone

Antimalarial

Mixed ligand complex

Single crystal

Zinc(II) complexes

ABSTRACT

Three novel mixed ligand Zn(II) complexes {complex **1** = [Zn(L1)₂(bpy)], complex **2** = [Zn(L2)₂(bpy)], complex **3** = [Zn(L2)₂(phen)]}, where bpy = 2,2'-bipyridine and phen = 1,10-phenanthroline of 4-(4-chlorobenzoyl)-2-(3-chlorophenyl)-5-methyl-2,4-dihydro-3H-pyrazol-3-one (HL1) and 4-(4-chlorobenzoyl)-5-methyl-2-(p-tolyl)-2,4-dihydro-3H-pyrazol-3-one (HL2) were synthesized and characterized by ¹H and ¹³C NMR, FTIR, TG-DTA, UV-Vis, elemental analysis, molar conductance and single crystal X-ray structure determination. Based on analytical and spectroscopic techniques, all the three Zn(II) complexes were found to have a distorted octahedral geometry. The ligands and the complexes were screened for antimalarial activity against *Plasmodium falciparum*. The zinc(II) complexes showed greater antimalarial activity than their parent ligands.

© 2020 Elsevier Ltd. All rights reserved.

1. Introduction

The two nitrogen atoms of an amidic ketone containing pyrazolone react with acid chlorides to give substitution on the 4th position of the pyrazolone, giving the commonly named 4-acyl pyrazolone. 4-Acyl pyrazolones have proven to be very useful in coordination chemistry as an -OO bidentate ligand [1–8]. There are reports in the literature on metal complexes of 4-acyl pyrazolones for d-block metals which display good antimalarial, anticancer, antibacterial, antifungal and catalytic activities.[2,6,8–11]

The lack of zinc can be a problem in biological systems and is responsible for various disease states [6,12]. Zinc has been used to reduce gastro toxicity, in which any extra drug binds to zinc and is released from the human body [13,14]. Malaria is an infectious disease caused by a parasite called *Plasmodium* and it is a serious problem for human health, especially in the so-called “Third World” [15]. The diseases are mainly caused by the main five parasite species: *Plasmodium falciparum*, *Plasmodium vivax*, *Plasmodium malariae*, *Plasmodium ovale* and *Plasmodium knowlesi* [16]. Amongst them, *Plasmodium falciparum* is the most deadly. Malaria is an entirely preventable and treatable mosquito-borne illness. However, drug resistance to currently available drugs increases multiple fold in the real world [17]. This prompted us

to explore better treatment for *Plasmodium falciparum*. Pyrazolone derivatives complexed with the zinc(II) metal have been investigated [18]. The current study explores 4-acyl pyrazolones and their zinc(II) complexes, which show promising antimalarial activity [4]. The studies performed using *in vitro* assays on *P. falciparum* strains with various concentrations of the metal complexes and ligands showed that the complexes were able to inhibit the parasite growth in a more effective manner than the parent compounds. With the same dose, the metal complexes showed greater activity than the ligands against malaria [4,19–22].

2. Experimental

2.1. Materials and methods

The pyrazolones were obtained from Sidhhanath Industries, Sachin (Surat), India as free gift samples. All necessary reagents and solvents were obtained from commercial sources. Zinc acetate, 2,2'-bipyridine and 1,10-phenanthroline were purchased from Spectrochem PVT. LTD., Mumbai. *P*-chloro benzoyl chloride was purchased from SRL Chemical, Mumbai.

Infrared (IR) spectra were recorded on a Bruker Alpha Fourier transform IR (FT-IR) spectrometer as KBr pellets. ¹H NMR spectra of the ligands were recorded with an AV 400 MHz Bruker FT-NMR instrument. Single crystal data were collected on a Bruker

* Corresponding author.

E-mail address: rjadeja-chem@msubaroda.ac.in (R.N. Jadeja).

CCD area-detector diffractometer. The electronic spectra were recorded on a Perkin Elmer Lambda 35 UV-Vis spectrometer. Simultaneous TG/DTA were carried out on an SII EXSTAR6000 TG/DTA 6300 instrument. The experiments were performed in N₂ at a heating rate of 10 °C min⁻¹ in the temperature range 30–550 °C using an aluminium pan. The purity of the ligands and their complexes was evaluated by thin-layer chromatography. Gravimetric and volumetric analyses were performed for the determination of zinc after decomposition of the complexes in nitric acid.

A local strain of *P. falciparum* from Gujarat State, India was cultured continuously according to the candle-jar method of Trager and Jensen (1976), *in vitro* in human red blood cells, with 5% haematocrit in RPMI (Roswell Park Memorial Institute) 1640 medium (Himedia Laboratories, India) supplemented with 25 mM HEPES (Himedia Laboratories, India), 0.23% sodium bicarbonate (Himedia Laboratories, India) and 10% heat-inactivated human O⁺serum.

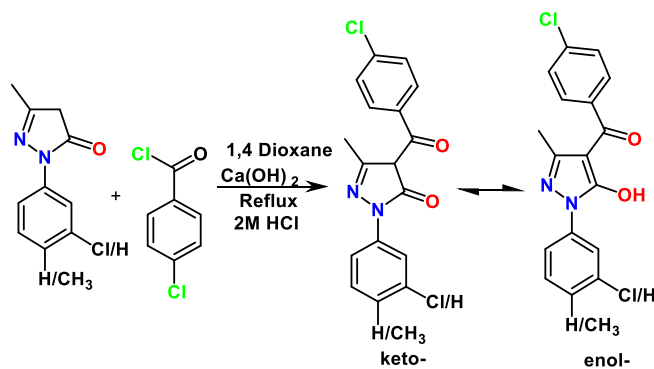
2.2. Synthesis of the ligands

2.2.1. Synthesis of 4-(4-chlorobenzoyl)-2-(3-chlorophenyl)-5-methyl-2,4-dihydro-3H-pyrazol-3-one [HL1]

The ligand synthesis was reported previously by us [3]. 2-(3-Chlorophenyl)-5-methyl-2,4-dihydro-3H-pyrazol-3-one (31.20 g, 0.1500 mol) was dissolved in 1,4-dioxane (120 ml) in a three necked 500 ml round bottom flask, with an addition funnel and reflux condenser attached. The reaction mixture was heated at 80 °C for 15 min. Calcium hydroxide (22.23 g, 0.3000 mol) was added, and after 10 min *p*-chloro benzoyl chloride (19.23 ml, 0.1500 mol) was added dropwise to the reaction mixture. The reaction mixture converted into a thick paste during this addition. After the complete addition, the reaction mixture was placed for reflux for 3 h. The reaction mixture was poured into a 300 ml solution of ice-cold hydrochloric acid (2 mol L⁻¹) under stirring. The colored precipitates that formed were filtered, washed with hot water and dried in a bulb oven. After drying, a pale yellow solid was obtained and recrystallized in rectified spirit [4]. Yield: 78%. Anal. Calcd for C₁₇H₁₂Cl₂N₂O₂ (%): C, 58.81; H, 3.48; N, 8.07; Found (%): C, 58.57; H, 3.71; N, 8.15. M.w.: 347.20. M.P.: 105 °C. Λ_m (S cm² mol⁻¹): 8.8. FTIR (KBr plates) ν (cm⁻¹): 1625 (s) (C=O, amide of pyrazolone), 1590 (m) (C=O, 4-chloro benzoyl), 966 (s) (N–N of pyrazolone), 1486 (m) (aromatic C–C). ¹H NMR (CDCl₃) δ ppm: 2.14 (s, 3H, pyrazolone C–CH₃), 7.28–7.30 (m, 1H, *m*-chloro Ph), 7.39–7.43 (m, 1H, *m*-chlorophenyl), 7.51–7.63 (m, 4H, *p*-chloro benzoyl), 7.83–7.85 (m, 1H, *m*-chloro Ph), 7.963–7.968 (m, 1H, *m*-chloro Ph). ¹³C NMR (CDCl₃) δ ppm: 16.01 (–CH₃–pyrazolone), 103.69 (C–pyrazolone ring), 118.35 (C–phenyl), 120.59 (C–phenyl), 126.66, 128.88, 129.47, 130.20, 134.93, 135.47 (C–Cl, *m*-chloro phenyl), 138.19 (C–Cl, *p*-chloro benzoyl), 138.46 (C–N, pyz with phenyl), 147.98 (C=N, pyrazolone ring), 162.02 (C–O, pyz), 190.13 (C=O, 4-chloro benzoyl).

2.2.2. Synthesis of 4-(4-chlorobenzoyl)-5-methyl-2-(*p*-tolyl)-2,4-dihydro-3H-pyrazol-3-one (HL2)

This ligand was reported in our recent publication [4]. Yield: 76%. Anal. Calcd for C₁₈H₁₅ClN₂O₂ (%): C, 66.16; H, 4.63; N, 8.57; Found (%): C, 66.11; H, 4.71, N, 8.77. M.w.: 326.78. M.P.: 108 °C. Λ_m (S cm² mol⁻¹): 10.1. IR (KBr, cm⁻¹): 1551 (C=N, cyclic), 1590 (C=O, 4-chloro benzoyl group) 1625 (m) (C=O, Pyrazolone ring); ¹H NMR (CDCl₃, 400 MHz) δ ppm: 2.1 (s, 3H, Pyrazolone C–CH₃), 2.38–2.39 (m, 1H, –CH–cyclic), 2.4 (s, 3H, CH₃–Ar), 7.28–7.30 (d, 2H, aromatic, *J* = 8 Hz), 7.50–7.52 (m, 2H, aromatic), 7.60–7.62 (d, 2H, *p*-chloro benzoyl-, *J* = 8 Hz), 7.72–7.74 (d, 2H, *p*-chloro benzoyl-, *J* = 8 Hz); ¹³C NMR (CDCl₃, 400 MHz) δ ppm: 15.90 (–CH₃, pyrazolone), 21.10 (–CH₃ tolyl), 103.37 (C–pyrazolone), 120.94, 128.79, 129.32, 129.72, 131.48, 134.59, 136.34, 136.87 (C–Cl,



Scheme 1. Synthesis route for ligands HL1 and HL2.

p-chloro benzoyl), 138.13 (C–N, pyz-phenyl), 147.54 (C=N, pyrazolone), 160.62 (C=O, C–O, pyz), 191.38 (C=O, 4-chloro benzoyl).

The synthesis of the ligands is summarized in Scheme 1.

2.3. Synthesis of the Zn(II) complexes

2.3.1. Synthesis of complex 1

In the synthesis procedure for complex 1, zinc acetate (1 mmol) was dissolved in a small amount of methanol and mixed with a methanolic solution of the ligand HL1 (2 mmol). After half an hour, a methanolic solution of 2,2'-bipyridine (1 mmol) was added dropwise. Subsequently, a small amount of sodium acetate was added and the reaction mixture placed on a stirrer. The reaction mixture was heated and reflux for 4 h [4]. The obtained light-yellow crystalline precipitates were filtered and washed with hot MeOH and hot water. A small amount of product was recrystallized from a DMF and ethanol mixture at room temperature. Yield: 64%. Anal. Calcd for C₄₄H₃₄Cl₄N₆O₄Zn (%): C, 57.57; H, 3.73; N, 9.16; Found (%): C, 56.58; H, 3.74; N, 9.22. Metal estimation, gravimetrically and volumetrically, Zn = 7.12%. M.w.: 917.97. M.P.: >210 °C. Λ_m (S cm² mol⁻¹): 9.9. FTIR (KBr plates) ν (cm⁻¹): 1621 (m) (C=O, 4-chloro benzoyl), 955 (s) (N–N of pyrazolone), 14,701 (m) (–C–C–aromatic), 493 (s) (O–M), 411 (s) (N–M). ¹H NMR (CDCl₃) δ ppm: 2.2 (s, 3H, pyrazolone C–CH₃), 7.0–7.34 (m, 2H, 3-chloro-phenyl), 7.64–7.67 (m, 2H, 4-chloro benzoyl), 7.77–7.79 (m, 1H, 4-chloro benzoyl), 8.01–8.08 (m, 1H, 3-chlorophenyl), 9.07–9.08 (d, 1H, *J* = 4 Hz, bpy), 8.22–8.24 (d, 1H, *J* = 8 Hz, bpy), 8.10–8.12 (t, 1H, *J* = 8 Hz, bpy). ¹³C NMR (CDCl₃) δ ppm: 16.56 (–CH₃–pyrazolone), 104.79 (C–pyz), 117.59, 119.51, 121.03, 124.06, 126.40, 128.27, 129.23, 129.53, 133.90, 136.21, 139.36, 139.91, 140.20, 148.99, 149.22 (C–N, pyz-phenyl), 149.63 (C=N, pyz), 166.93 (C–O, pyz), 190.04 (C=O, *p*-chloro benzoyl).

2.3.2. Synthesis of complex 2

Complex 2 was synthesized by dissolving zinc acetate (1 mmol) in methanol followed by the addition of a methanolic solution of the ligand HL2 (2 mmol). After half an hour, 2,2'-bipyridine (1 mmol) was added to the reaction mixture, followed by refluxing for 4 h. After this, the reaction mixture gave a light yellowish crystalline product. The product was filtered with a Whatman filter paper, washed with 10 ml methanol and then with hot water. A small amount of the product was recrystallized from DMF at room temperature [4]. Yield: 85.2%. Anal. Calcd for C₄₆H₃₆Cl₂N₆O₄Zn (%): C, 63.28; H, 4.16; N, 9.63; Found (%): C, 63.21, H, 4.23, N, 9.68. Metal estimation, gravimetrically and volumetrically, Zn = 7.49%. M.w.: 873.11. M.P.: >210 °C. Λ_m (S cm² mol⁻¹): 10.5. FTIR (KBr, cm⁻¹): 1629 (C=O, 4-chloro benzoyl group), 1597 (C=N, cyclic), 943 (s) (N–N), 1435 (s) (Ar–C–C). ¹H NMR (CDCl₃, 400 MHz) δ ppm: 1.6 (s, 3H, CH₃–CAr), 2.2 (s, 3H, Pyz–CC–CCH₃), 6.99–

7.02 (d, 2H, aromatic-H, $J = 8$ Hz), 7.57–8.2 (m, 6H, *ar*-H), 9.00–9.02 (d, 1H, $J = 8$ Hz, bpy).

2.3.3. Synthesis of complex 3

The procedure for the preparation of complex **3** is similar to that for complex **2**, except that 2,2'-bipyridine was replaced with 1,10-phenanthroline. Complex **3** was recrystallized from a DMF and ethanol mixture at room temperature [4]. Yield: 86.7%. Anal. Calcd for $C_{48}H_{40}Cl_2N_6O_4Zn$ (%): C, 63.98; H, 4.47; N, 9.33; Found (%): C, 64.01, H, 4.55; N, 9.65. M.w.: 901.17. M.P.: >200 °C. Λ_m ($S\ cm^{-2}\ mol^{-1}$): 9.7. Metal estimation, gravimetrically and volumetrically, Zn = 7.26%. FTIR (KBr, cm^{-1}): 1562 (C=N, cyclic), 1622 (C=O, 4-chloro benzoyl group), 943 (s) (N–N), 1436 (s) (Ar–C–C). 1H NMR ($CDCl_3$, 400 MHz) δ ppm: 1.6 (s, 3H, CH_3 -tolyl), 2.2 (s, 3H, Pyz-C- CH_3), 6.99–7.02 (d, 2H, aromatic-H, $J = 8$ Hz), 7.24–7.31 (m, 2H, *ar*-H), 7.60–7.62 (d, 2H, aromatic-H, $J = 8$ Hz), 7.72–7.74 (d, 2H, 4-chloro benzoyl-, $J = 8$ Hz), 9.30–9.31 (m, 1H, aromatic), 8.49–8.51 (m, 1H, phen). The synthesis route for complexes **1–3** is summarized in Scheme 2.

2.4. X-ray structure determination

The single crystal X-ray crystallographic data for the ligands (HL1 and HL2) and the complexes (**1**, **2** and **3**) are summarized in Table 1. The single crystal crystallographic data were collected on a Bruker CCD area-detector diffractometer with graphite monochromated $MoK\alpha$ radiation ($\lambda = 0.71073$ Å). The Mercury software package was used for the ORTEP views of the ligands and the complexes and these are given in Fig. 1. All structures were solved by direct methods, using SHELXS97 [23]. All non-hydrogen atoms of the molecules were located in the expected positions in the obtained structures. For the refinement, full-matrix least-squares refinement was carried out using SHELXL97 [24]. All hydrogen atoms were included as idealized atoms riding on their respective carbon atoms with C–H bond lengths appropriate to the carbon atom hybridization [25,26].

2.5. *P. falciparum* in vitro growth inhibition assay

The *in vitro* antimalarial assay was performed as described by Rieckmann et al., (1978) with minor modifications [27]. The *P. falciparum* cultures were synchronized by treatment with 5% D-sorbitol (Himedia Laboratories, India) to obtained ring stage parasitized cells (Lambros and Vanderberg, 1979) [28]. For the assay, an initial ring stage parasitaemia of 0.8 to 1.5% at 3% haematocrit in a total volume of 200 μ l of medium RPMI-1640 deter-

mined by JSB staining (Sing, 1956) was used to assess the percent parasitaemia (rings) and uniformly maintained with 50% RBCs (O^+) [29]. A stock solution of 5 mg/ml of each of the test samples was prepared in DMSO and subsequent dilutions were prepared with the culture medium. The diluted samples of 20 μ l volume were added to the test wells containing the parasitized cell preparation to obtain final concentrations (at five-fold dilutions), ranging from 0.4 to 100 μ g/ml. The culture plates were incubated at 37 °C in a candle jar. After 36–40 h incubation, thin blood smears from each well were prepared and stained with JSB stain. The slides were microscopically observed to record the maturation of the ring-stage parasites into trophozoites and schizonts in the presence of different concentrations of the test agents. The test concentration which inhibited the complete maturation into schizonts was recorded as the minimum inhibitory concentration (MIC). Chloroquine was used as the reference drug (Fig. 2).

3. Results and discussion

3.1. Crystal structures of the ligands and complexes

The crystallographic data of the two ligands (HL1 and HL2) and the three complexes **1–3** are given in Table 1. The structures with atom numbering schemes are represented in Fig. 1. Selected bond length and bond angles of the ligands (HL1 and HL2) and complexes **1–3** are given in Tables 2 and 3.

3.1.1. Crystal structure of the ligand HL1

In the ligand, the C8–O1 (1.243 Å) and C11–O2 bonds (1.222 Å) have lengths that are near to typical C–O double bond lengths [11,30]. The bond length of C7–C8 is 1.427 Å, near to a typical C–C single bond length, and the bond length of C8–C9 is 1.390 Å near to a typical C–C double bond length. Furthermore the C7–N1 bond (1.310 Å) is longer than a C–N double bond and since an H atom is attached to the N atom, this reveals that the ligand is present in the NH amino diketone form [11,30]. Selected bond lengths and bond angles for the ligand are given in Table 2.

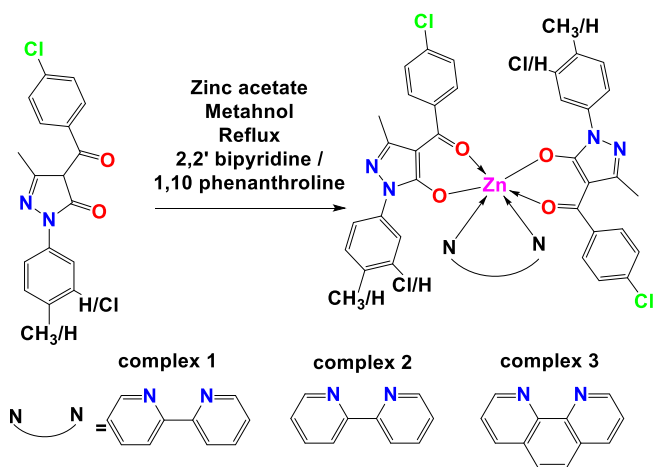
There is intermolecular hydrogen bonding between the –NH group of one molecule and the carbonyl (C=O) group of the pyrazolone ring of a second molecule of the ligand. The parameters (D–H...A) are as follows: N2–H2 (0.860 Å), H2...O1 (1.790 Å), N2–O1 (2.631 Å) and N2–H2–O1 (165.51°). The stability of the NH amino diketone form may be due to the presence of the intermolecular hydrogen bonding. Furthermore, in the crystal packing system, the molecule arrangement design appears as zigzag lines from the 'b' axis (Fig. 3).

3.1.2. Crystal structure of the ligand HL2

In the ligand HL2, the crystal data show two molecules of HL2 in the same plane. Selected bond length and bond angles are presented in Table 2. There is intramolecular hydrogen bonding between the –OH group of one molecule and the carbonyl (C=O) group of the same ligand. The parameters (D–H...A) are as follows: O1–H1 (0.820 Å), H1...O2 (1.811 Å), O1–O2 (2.501 Å) and O1–H1...O2 (140.84°) (Fig. 4).

3.1.3. Crystal structure of $[Zn(L1)_2(bpy)]$ (complex 1)

The single crystal X-ray analysis for complex **1** gives the general structural formula ML_2L' (where L = L1 and L' = 2,2'-bipyridine). The zinc(II) ion is hexacoordinated by four oxygen atoms (O1, O2, O3 and O4) of two acyl pyrazolone ligands (L1) and two nitrogen atoms (N5 and N6) of the 2,2'-bipyridine ligand. The structure of complex **1** is illustrated in Fig. 1. Selected bond lengths and bond angles are listed in Table 3. The coordination geometry is styled as octahedral. Two oxygen atoms [O(2) and O(3)] from two HL1



Scheme 2. Synthesis route for mixed ligand complexes **1–3**.

Table 1
Crystal data and structure refinement for HL1, HL2, and complexes 1–3.

Identification code	HL1	HL2	Complex 1	Complex 2	Complex 3
Empirical formula	C ₁₇ H ₁₁ Cl ₂ N ₂ O ₂	C ₁₈ H ₁₅ Cl ₁ N ₂ O ₂	C ₄₄ H ₃₀ Cl ₄ N ₆ O ₄ Zn	C ₄₉ Cl ₂ N ₇ O ₅ Zn	C ₅₁ H ₄₂ Cl ₂ N ₇ O ₅ Zn
Formula weight	346.18	326.77	913.91	902.83	969.18
Temperature/K	293	293	293	293	293
Crystal system	Monoclinic	Triclinic	Triclinic	Monoclinic	Triclinic
Space group	<i>P</i> 2 ₁ / <i>c</i>	<i>P</i> -1	<i>P</i> -1	<i>P</i> 2 ₁ / <i>n</i>	<i>P</i> -1
<i>a</i> /Å	15.1886(17)	7.9800(6)	9.0491(4)	12.5956(6)	13.4212(8)
<i>b</i> /Å	9.6726(7)	11.6196(6)	12.6789(6)	26.5655(10)	13.7150(8)
<i>c</i> /Å	11.8403(12)	18.0179(9)	18.7081(6)	14.6544(7)	14.0396(7)
α /°	90	84.835(4)	82.155(3)	90	88.005(4)
β /°	112.599(13)	78.544(5)	79.592(3)	110.822(5)	80.209(4)
γ /°	90	72.202(6)	81.754(4)	90	66.901(5)
Volume/Å ³	1605.9(3)	1558.28(17)	2075.78(15)	4583.2(4)	2341.0(2)
<i>Z</i>	4	2	2	4	2
$\rho_{\text{calc}}/\text{cm}^{-3}$	1.432	1.393	1.462	1.308	1.375
μ/mm^{-1}	0.414	0.256	0.900	0.705	0.694
<i>F</i> (0 0 0)	708.0	680.0	932.0	1788.0	1002.0
Crystal size/mm ³	0.3 × 0.2 × 0.2	0.3 × 0.2 × 0.2	0.3 × 0.2 × 0.2	0.3 × 0.2 × 0.2	0.3 × 0.2 × 0.2
Radiation(Å)	MoK α (λ = 0.71073)	MoK α (λ = 0.71073)	MoK α (λ = 0.71073)	MoK α (λ = 0.71073)	MoK α (λ = 0.71073)
The 2 θ range for data collection/°	6.882 to 57.73	5.996 to 58.014	6.506 to 58.424	6.144 to 58.722	6.19 to 58.224
Index ranges	−17 ≤ <i>h</i> ≤ 20, −5 ≤ <i>k</i> ≤ 13, −16 ≤ <i>l</i> ≤ 8	−10 ≤ <i>h</i> ≤ 10, −15 ≤ <i>k</i> ≤ 15, −24 ≤ <i>l</i> ≤ 24	−12 ≤ <i>h</i> ≤ 11, −17 ≤ <i>k</i> ≤ 17, −25 ≤ <i>l</i> ≤ 25	−16 ≤ <i>h</i> ≤ 16, −36 ≤ <i>k</i> ≤ 36, −19 ≤ <i>l</i> ≤ 18	−18 ≤ <i>h</i> ≤ 17, −18 ≤ <i>k</i> ≤ 18, −19 ≤ <i>l</i> ≤ 19
Reflections collected	5321	33,561	45,888	51,601	51,456
Independent reflections	3299 [<i>R</i> _{int} = 0.0211, <i>R</i> _{sigma} = 0.0350]	7546 [<i>R</i> _{int} = 0.0433, <i>R</i> _{sigma} = 0.0477]	10,074 [<i>R</i> _{int} = 0.0450, <i>R</i> _{sigma} = 0.0441]	11,254 [<i>R</i> _{int} = 0.0873, <i>R</i> _{sigma} = 0.0834]	11,368 [<i>R</i> _{int} = 0.1462, <i>R</i> _{sigma} = 0.1772]
Data/11368/0/601	restraints/parameters	3299/0/209	7546/0/420	10074/0/534	11254/0/577
Goodness-of-fit on <i>F</i> ²	1.045	1.319	1.030	1.039	1.007
Final <i>R</i> indexes [<i>i</i> > 2 σ (<i>I</i>)]	<i>R</i> ₁ = 0.0546, <i>wR</i> ₂ = 0.1319	<i>R</i> ₁ = 0.0729, <i>wR</i> ₂ = 0.2059	<i>R</i> ₁ = 0.0469, <i>wR</i> ₂ = 0.0932	<i>R</i> ₁ = 0.0814, <i>wR</i> ₂ = 0.2186	<i>R</i> ₁ = 0.0718, <i>wR</i> ₂ = 0.1206
Final <i>R</i> indexes [all data]	<i>R</i> ₁ = 0.0880, <i>wR</i> ₂ = 0.1470	<i>R</i> ₁ = 0.1227, <i>wR</i> ₂ = 0.2383	<i>R</i> ₁ = 0.0867, <i>wR</i> ₂ = 0.1098	<i>R</i> ₁ = 0.1519, <i>wR</i> ₂ = 0.2646	<i>R</i> ₁ = 0.2135, <i>wR</i> ₂ = 0.1701
Largest diff. peak/hole/e Å ^{−3}	0.42/−0.48	1.29/−0.76	0.47/−0.55	0.58/−0.48	0.39/−0.34

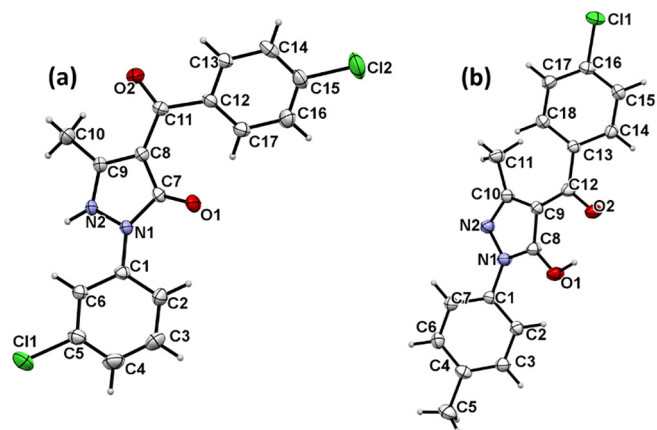


Fig. 1A. ORTEP diagrams of the ligands with 40% probability ellipsoids (a) HL1 and (b) HL2.

ligands and two nitrogen atoms [N(5) and N(6)] from the 2,2'-bipyridine ligand comprise the equatorial planes. The deviations of the coordination atoms O(2), O(3), N(5) and N(6) from the mean plane are 0.0073, 0.069, 0.077 and 0.081 Å, respectively. The Zn(II) metal ion strays from the equatorial plane by 0.008 Å. The coordination plane around the Zn(1) ion is composed of the O(2), O(3), N(5) and N(6) atoms and the regular bond distances for Zn(1)—O(2), Zn(1)—O(3), Zn(1)—N(5) and Zn(1)—N(6) are 2.069(15), 2.061(17), 2.150(2) and 2.140(2) Å, respectively. Two oxygen atoms [O(1) and O(4)] of the HL1 ligands are in axial positions, with the distance from the equatorial plane being 2.109 and 2.129 Å, respectively [3,4]. The O(2)—Zn(1)—N(5), O(3)—Zn(1)—N(6) and O(1)—Zn(1)—

O(4) angles are 167.91(7), 174.87(7) and 175.91(6)°, respectively, which are deviated from the theoretical value of 180° for the proper geometric structure. The O(2)—Zn(1)—O(1), O(3)—Zn(1)—O(1), O(1)—Zn(1)—N(5), O(1)—Zn(1)—N(6), O(2)—Zn(1)—O(4), O(3)—Zn(1)—O(4), O(4)—Zn(1)—N(5) and O(4)—Zn(1)—N(6) angles are 86.65(6), 90.15(7), 89.10(7), 93.57(7), 91.67(6), 86.13(7), 100.59(8) and 90.25(7)° respectively, which are deviated from the 90° angle between the axial line and equatorial plane. Therefore, the local coordination geometry around the zinc ion in the complex is distorted octahedral (Fig. 5) [4,6,31].

3.1.4. Crystal structure of [Zn(L2)₂(bpy)] (complex 2)

Complex 2 contains the 2,2'-bipyridine ligand together with two acyl pyrazolone (HL2) ligands. Selected bond lengths and bond angles of complex 2 are presented in Table 2. The single crystal X-ray analysis for complex 2 shows the general structural formula M(L2)₂L' (where L' is 2,2'-bipyridine). The zinc(II) ion is hexacoordinated by four oxygen atoms (O1, O2, O3 and O4) of the two acyl pyrazolone ligands (L2) and two nitrogen atoms (N5 and N6) of the 2,2'-bipyridine ligand. The structure of complex 2 is illustrated in Fig. 1. Two oxygen atoms [O(1) and O(3)] from the two HL2 ligands and two nitrogen atoms [N(5) and N(6)] from the 2,2'-bipyridine ligand create the equatorial plane. The deviations of the coordination atoms O(1), O(3), N(5) and N(6) from the mean plane are 0.128, 0.131, 0.157 and 0.154 Å, respectively. The Zn(II) metal ion strays from the equatorial plane by 0.015 Å. The coordination plane around the Zn(1) ion is composed of the O(1), O(3), N(5) and N(6) atoms and the regular bond distances for Zn(1)—O(1), Zn(1)—O(3), Zn(1)—N(5) and Zn(1)—N(6) are 2.071(3), 2.064(3), 2.126(4) and 2.111(4) Å, respectively. Two oxygen atoms [O(2) and O(4)] of the HL2 ligands are in axial positions with the distance

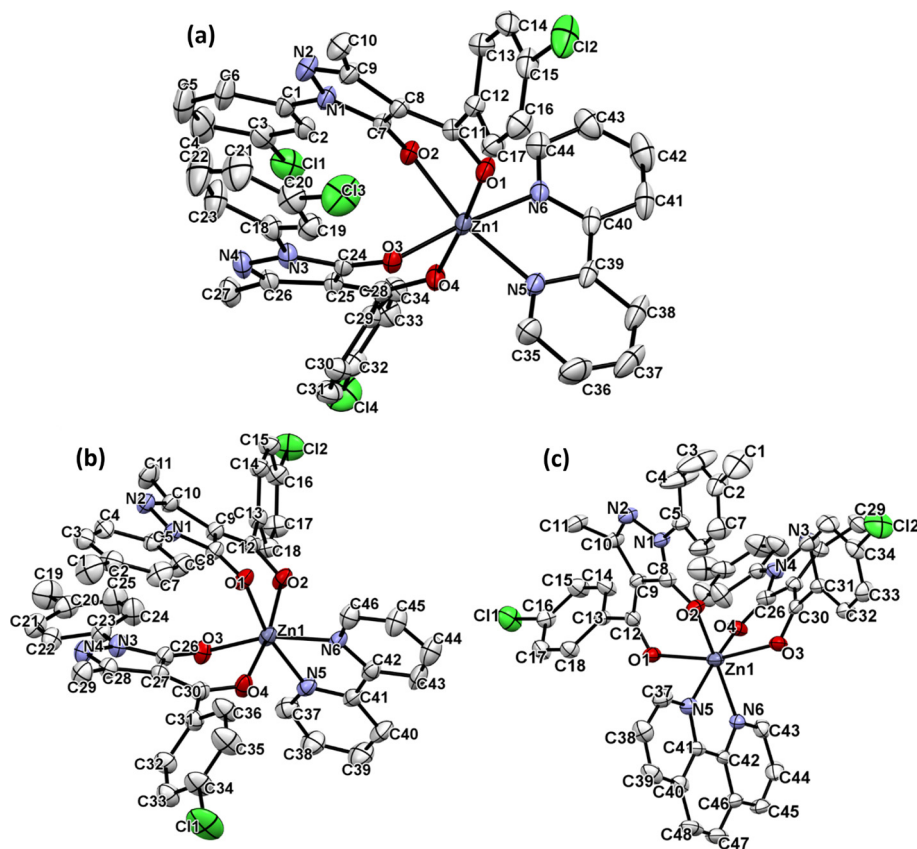


Fig. 1B. ORTEP diagrams with 40% probability ellipsoids (a) complex 1, (b) complex 2 and (c) complex 3. Hydrogen atoms and solvent molecules have been omitted for clarity.

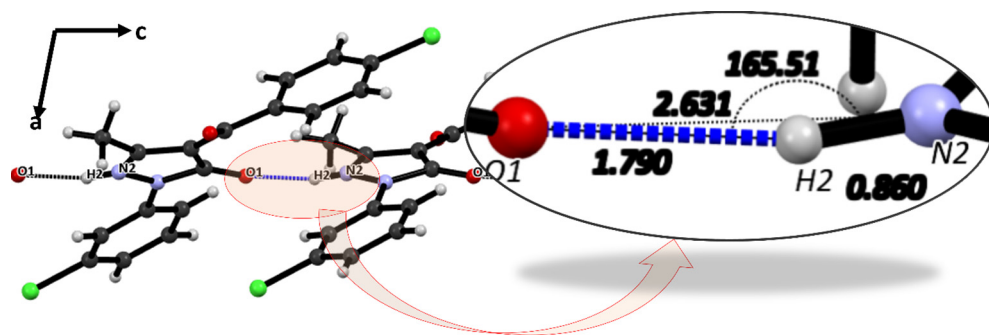


Fig. 2. Intermolecular H-bond in HL1 viewed down the 'b' axis.

from the equatorial plane being 2.144 and 2.080 Å respectively [3,4]. The O(1)—Zn(1)—N(5), O(3)—Zn(1)—O(4) angles are 168.02(14), 164.78(15) and 170.44(13)°, respectively, which are deviated from the theoretical value of 180° for the proper geometric structure. The O(2)—Zn(1)—O(1), O(3)—Zn(1)—O(1), O(2)—Zn(1)—N(5), O(2)—Zn(1)—N(6), O(1)—Zn(1)—O(4), O(3)—Zn(1)—O(4), O(4)—Zn(1)—N(5) and O(4)—Zn(1)—N(6) angles are 83.89(13), 98.68(13), 89.83(14), 99.07(14), 88.20(14), 85.69(14), 98.89(15) and 86.83(14)°, respectively, which are deviated from the 90° angle between the axial line and the equatorial plane. Therefore, the geometry around the zinc ion in the complex is distorted octahedral (Fig. 5) [4,6,31].

3.1.5. Crystal structure of [Zn(L2)₂(phen)] (complex 3)

The mixed ligand complex 3 has 1,10-phenanthroline as a secondary ligand in its structure. Selected bond lengths and bond angles are illustrated in Table 3. In the geometry of complex 3,

two oxygen atoms, O(2) and O(3), of each 4-acyl pyrazolone (L2) ligand are in the equatorial plane together with two nitrogen atoms of the 1,10-phenanthroline ligand. The deviations of the coordination atoms O(2), O(3), N(5) and N(6) from the mean plane are 0.108, 0.111, 0.130 and 0.131 Å, respectively. The Zn(II) metal ion strays from the equatorial plane by 0.018 Å. The coordination plane around the Zn(II) ion is composed of the O(2), O(4), N(5) and N(6) atoms and the regular bond distances for Zn(1)—O(2), Zn(1)—O(4), Zn(1)—N(5) and Zn(1)—N(6) are 2.042(3), 2.144(4) and 2.154(3) Å, respectively [4,32,33]. Two oxygen atoms, O(1) and O(3), of the acyl pyrazolone (L2) ligands are in axial positions. The O(2)—Zn(1)—N(6), O(4)—Zn(1)—N(5) and O(1)—Zn(1)—O(3) angles are 166.95(13), 164.65(12) and 163.50(10)°, respectively. These angles are deviated from the theoretical value of 180° for the proper geometric structure. The O(4)—Zn(1)—O(2), O(4)—Zn(1)—N(6), N(5)—Zn(1)—N(6), O(2)—Zn(1)—N(5), O(1)—Zn(1)—O(4), O(3)—Zn(1)—O(4), O(1)—Zn(1)—N(5) and O(3)—Zn(1)—

Table 2
Selected bond angles and bond lengths for the ligands HL1 and HL2.

HL1			
Atoms	Length/Å	Atoms	Angle/°
C1—C5	1.747(3)	C9—N2—N1	110.20(18)
C12—C15	1.740(3)	N2—N1—C7	108.42(19)
O1—C7	1.243(3)	N2—N1—C1	120.21(18)
N2—N1	1.366(3)	C7—N1—C1	130.7(2)
N2—C9	1.314(3)	O1—C7—N1	121.4(2)
N1—C7	1.394(3)	O1—C7—C8	133.1(2)
N1—C1	1.414(3)	N1—C7—C8	105.4(2)
O2—C11	1.222(3)	N2—C9—C8	109.2(2)
C7—C8	1.427(4)	N2—C9—C10	119.7(2)
C9—C8	1.391(3)	C8—C9—C10	131.1(2)
C9—C10	1.481(4)	C7—C8—C11	129.6(2)
C8—C11	1.460(4)	C9—C8—C7	106.8(2)
C1—C6	1.386(3)	C9—C8—C11	123.5(2)
HL2			
Atoms	Length/Å	Atoms	Angle/°
O1—C8	1.310(3)	C10—N2—N1	106.1(2)
O2—C12	1.261(3)	N2—N1—C1	120.0(2)
C9—C10	1.427(4)	C8—N1—N2	110.4(2)
C9—C8	1.403(4)	C8—N1—C1	129.5(2)
C9—C12	1.431(4)	C17—C16—C11	119.0(2)
C10—C11	1.504(4)	C15—C16—C11	119.5(2)
N2—N1	1.396(3)	C15—C16—C17	121.5(3)
N2—C10	1.312(3)	C14—C13—C12	118.7(2)
N1—C1	1.423(3)	C14—C13—C18	119.1(2)
N1—C8	1.336(3)	C2—C1—N1	120.5(2)
C11—C16	1.736(3)	O1—C8—C9	127.9(2)

N(6) angles are 101.76(12), 90.37(13), 76.73(14), 91.90(13), 83.87(11), 87.02(11), 90.08(12) and 94.03(11)°, respectively, which are deviated from the 90° angle between the axial line and equatorial plane. Therefore the geometry around the zinc ion in the complex is distorted octahedral (Fig. 5) [3,4,6].

3.2. ¹H and ¹³C NMR spectra

The synthesized ligands HL1 and HL2 have been characterized by their ¹H and ¹³C NMR spectra in CDCl₃. The spectra are in good agreement with the proposed structures of the ligands. In the ¹H NMR spectrum of HL1, a singlet appears at δ 2.13 ppm for the methyl protons of the 3-methyl pyrazolone. The ligand shows multiplets in the region δ 7.3–7.9 ppm, corresponding to the aromatic protons. In the ¹H NMR spectrum of HL2, there are two singlets at δ 2.13 and 2.39 ppm, corresponding to methyl protons of CH₃-pyrazolone and tolyl pyrazolone, respectively. The peaks for the aromatic protons of the acyl pyrazolone are observed in the range δ 7.3–7.7 ppm (Fig. 6).

In the ¹³C NMR spectra of the ligands, there are fifteen signals observed for HL1 and fourteen signals observed for HL2. The carbon atoms of the methyl group of the pyrazolone ring appeared at δ 16.01 and 15.90 ppm for HL1 and HL2, respectively. The methyl group of tolyl group of HL2 appears at δ 21.10 ppm. The signals of the carbonyl carbon atom of the *p*-chloro benzoyl group are observed at δ 190 and 191 ppm for HL1 and HL2, respectively. In the range δ 103–148 ppm, signals are found for the aromatic rings of the pyrazolone and *p*-chloro benzoyl groups for both ligands (Fig. 7).

In the ¹H NMR spectrum of complex 1, the proton signal of the methyl group of pyrazolone is observed at δ 1.6 ppm. The aromatic protons of the acyl pyrazolone ligand are observed between δ 7 and 8 ppm. A triplet and two doublets for the aromatic protons of the 2,2'-bipyridine ligand are observed in the range δ 8–9.1 ppm [4,6].

Table 3
Selected bond angles and bond lengths for complexes 1–3.

Complex 1			
Atoms	Length/Å	Atoms	Angle/°
Zn1—O4	2.1225(16)	O4—Zn1—N6	90.25(7)
Zn1—O3	2.0610(17)	O4—Zn1—N5	93.26(7)
Zn1—O1	2.1187(16)	O3—Zn1—O4	86.13(7)
Zn1—O2	2.0693(15)	O3—Zn1—O1	90.15(7)
Zn1—N6	2.140(2)	O3—Zn1—O2	90.74(6)
Zn1—N5	2.150(2)	O3—Zn1—N6	174.87(7)
C12—C15	1.740(3)	O3—Zn1—N5	100.59(8)
C11—C3	1.740(3)	O1—Zn1—O4	175.91(6)
C14—C32	1.743(3)	O1—Zn1—N6	93.57(7)
O4—C28	1.263(3)	O1—Zn1—N5	89.10(7)
O3—C24	1.273(3)	O2—Zn1—O4	91.67(6)
O1—C11	1.266(3)	O2—Zn1—O1	86.65(6)
O2—C7	1.270(3)	O2—Zn1—N6	93.00(7)
Complex 2			
Atoms	Length/Å	Atoms	Angle/°
Zn1—O2	2.138(3)	O3—Zn1—O2	90.21(14)
Zn1—O3	2.064(3)	O3—Zn1—O1	98.68(13)
Zn1—O1	2.071(3)	O3—Zn1—O4	85.69(14)
Zn1—O4	2.103(3)	O3—Zn1—N5	91.52(15)
Zn1—N5	2.126(4)	O3—Zn1—N6	164.78(15)
Zn1—N6	2.111(4)	O1—Zn1—O2	83.89(13)
C12—C16	1.734(5)	O1—Zn1—O4	88.20(14)
C11—C34	1.732(6)	O1—Zn1—N5	168.02(14)
O2—C12	1.265(5)	O1—Zn1—N6	94.31(14)
O3—C26	1.267(6)	O4—Zn1—O2	170.44(13)
		O4—Zn1—N5	98.89(15)
Complex 3			
Atoms	Length/Å	Atoms	Angle/°
Zn1—O3	2.160(3)	O3—Zn1—O1	163.50(10)
Zn1—O2	2.042(3)	O2—Zn1—O3	81.95(11)
Zn1—O1	2.160(3)	O2—Zn1—O1	86.47(11)
Zn1—O4	2.034(3)	O2—Zn1—N6	166.95(13)
Zn1—N6	2.154(3)	O2—Zn1—N5	91.90(13)
Zn1—N5	2.144(4)	O4—Zn1—O3	87.02(11)
C11—C16	1.744(4)	O4—Zn1—O2	101.76(12)
C12—C34	1.734(4)	O4—Zn1—O1	83.87(11)
O3—C30	1.260(4)	O4—Zn1—N6	90.37(13)
O2—C8	1.262(5)	O4—Zn1—N5	164.65(12)
O1—C12	1.268(5)	N6—Zn1—O3	94.03(11)
O4—C26	1.272(4)	N6—Zn1—O1	99.74(11)

In the ¹H NMR spectrum of complex 2, there are two singlets at δ 1.6 and 2.2 ppm for the methyl and tolyl groups of the HL2 ligand. Multiplet signals in the aromatic region are observed which correspond to the aromatic protons of the HL2 and 2,2'-bipyridine ligands [4,6].

In the ¹H NMR spectrum of complex 3, the methyl group of pyrazolone gives a signal at δ 1.66 ppm and a singlet for the tolyl protons is observed at δ 2.28 ppm. The aromatic protons of the acyl pyrazolone and 1,10-phenanthroline ligands are observed in the range δ 7–9 ppm [4,6].

In the ¹³C NMR spectrum of complex 1, twenty NMR signals have been observed, which are in complete agreement with the total number of carbon atoms in this Zn(II) complex. In complex 1, the carbonyl carbon atom of *p*-chloro benzoyl and one carbon atom (C—O—) of the pyrazolone ring are observed at δ 190 and 166 ppm, respectively [4,6]. The ¹H and ¹³C NMR spectra of the ligands and the complexes are presented in the supporting information (S1–S8) (Fig. 8).

3.3. IR spectroscopy

The FT-IR spectrum of the ligand HL1 shows bands at 3426, 1625 and 1590 cm⁻¹, which can be assigned to νN—H, νCO (amide) and νCO (ketone), respectively. The HL1 ligand band at 1173 cm⁻¹

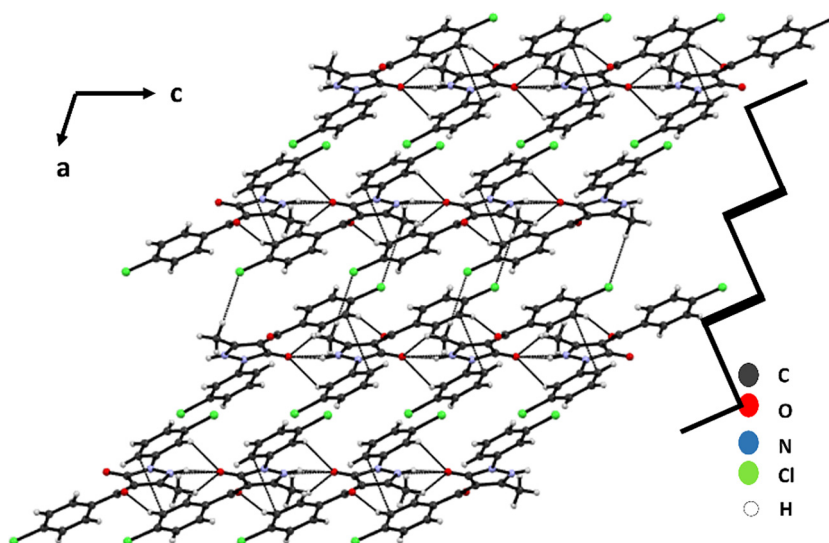


Fig. 3. Zigzag view of the crystal packing of the HL1 molecule viewed down the 'b' axis. Thin black lines indicate short contacts in the crystal packing.

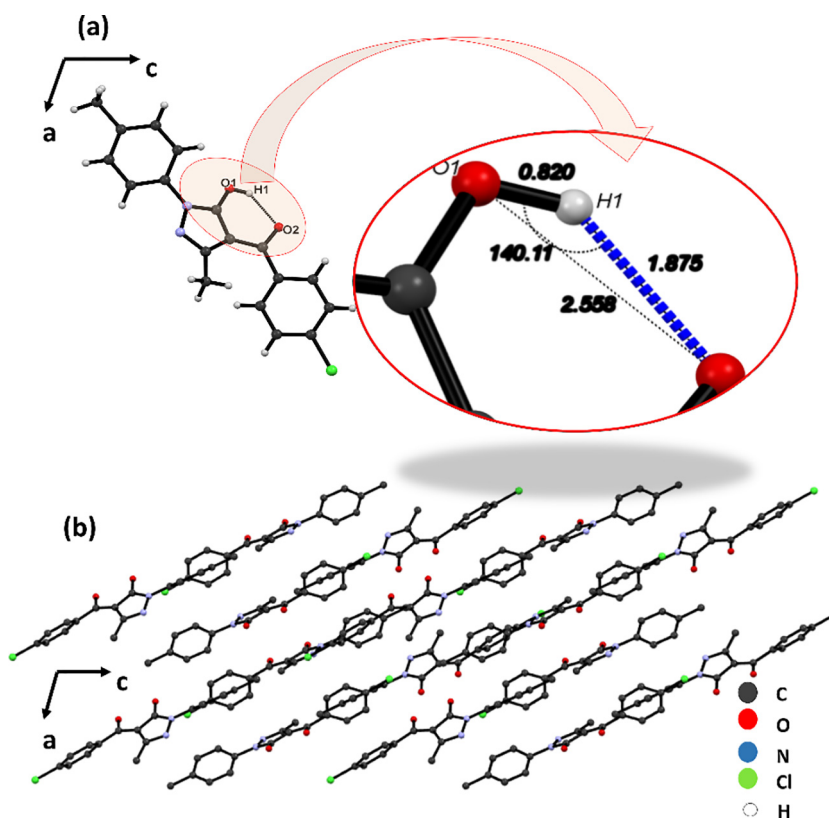


Fig. 4. (a) Intramolecular H-bond in the HL2 ligand, viewed down the 'a' axis. (b) Parallel arrangement of molecules in the crystal packing of the ligand HL2.

may be attributed to ν_{C-N} . Similarly, the ligand HL2 exhibits bands at 3441, 1625 and 1590 cm^{-1} which can be assigned to ν_{N-H} , ν_{CO} (amide) and ν_{CO} (ketone), respectively [4,11].

Complex 1 shows an absorption at 1625–1621 cm^{-1} , assigned to ν_{CO} . In comparison with the ligand's spectrum, this band is shifted to a lower wavelength, which may be due to the interaction with the metal ion. Complex 1 shows bands at 471 and 439 cm^{-1} due to ν_{M-O} and ν_{M-N} , respectively [3,4,6,12].

In the FTIR spectrum of complex 2, absorptions are observed at 1626 and 1564 cm^{-1} due to ν_{CO} (ketone) and $\nu_{C=N}$, respectively. New bands were observed at 476 and 415 cm^{-1} due to $\nu(\text{Zn-O})$ and $\nu(\text{Zn-N})$, respectively [4,8,11].

Complex 3 exhibited bands at 1622 and 1562 cm^{-1} due to ν_{CO} (ketone) and $\nu_{C=N}$, respectively. New bands were observed at 476 and 424 cm^{-1} due to ν_{M-O} and ν_{M-N} , respectively. A comparison between the FT-IR spectra of the ligands and the com-

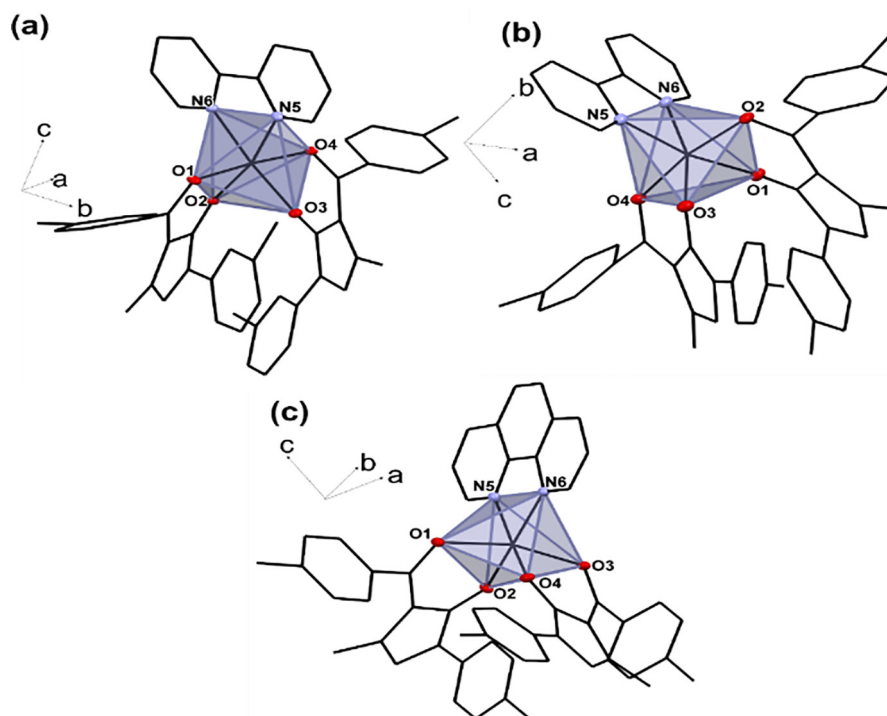


Fig. 5. Distorted octahedral geometry of all the zinc(II) complexes (a) complex **1**, (b) complex **2** and (c) complex **3**. Structures are in wireframe with a polyhedral style.

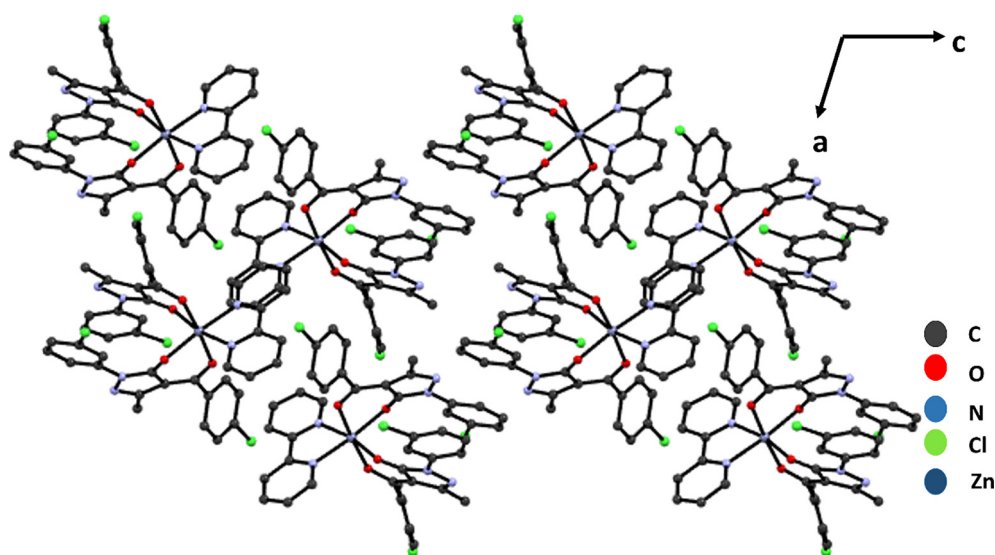


Fig. 6. Crystal packing viewed down the 'a' axis of complex **1**. The bipyridyl rings are arranged parallel to each other.

plexes revealed that complexes **1** and **3** contain 2,2'-bipyridine and 1,10-phenanthroline, respectively, with the corresponding acyl pyrrolone ligands [4,8,11]. The FTIR spectra are presented in the supporting information (S9–S13).

3.4. Electronic spectral studies

The electronic spectra of the ligands HL1 and HL2 and their zinc complexes **1**, **2** and **3** were recorded in DMSO (Fig. 9). In the spectra of the Zn(II) complexes, no d-d bands were observed, as expected

for a d^{10} configuration. A broad band in the region 320–400 nm may be attributed to a ligand to metal charge transfer [3,4].

3.5. Thermogravimetric analysis.

3.5.1. TGA of $[Zn(L1)_2(bpy)]$ (complex **1**)

The TGA graph of complex **1** showed the complex was air stable and it had high thermal stability (Fig. 10). The thermal study was carried out using the thermogravimetric technique with a heating rate of $10\text{ }^\circ\text{C min}^{-1}$. Slowly degradation started up to $250\text{ }^\circ\text{C}$, which

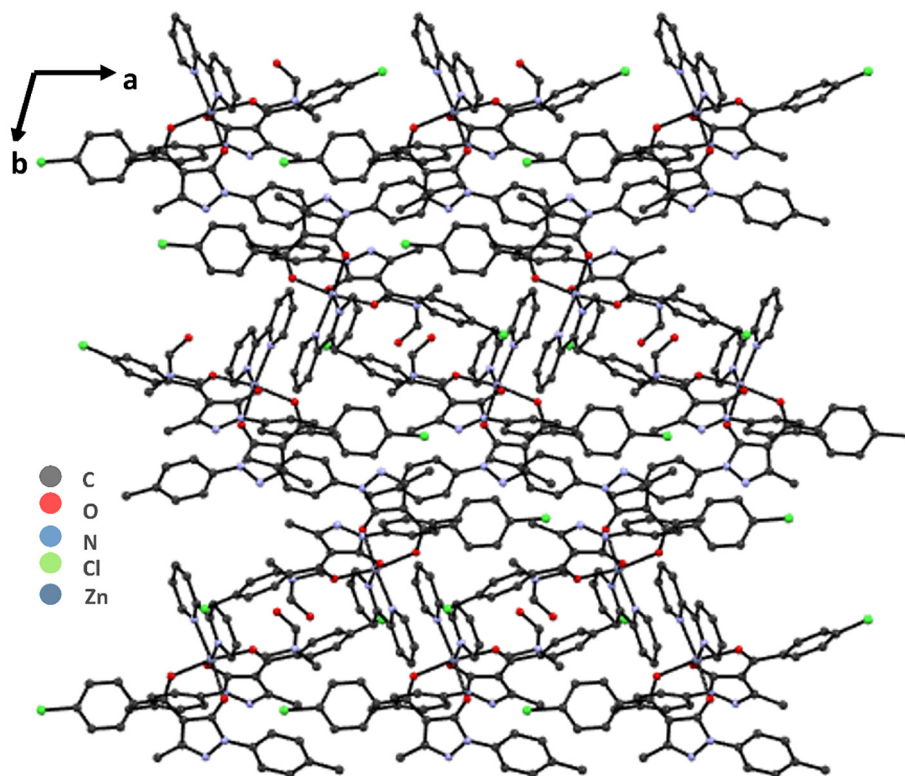


Fig. 7. Crystal packing viewed down the 'c' axis of complex 2. The bipyrindyl rings are arranged parallel to each other in complex 2.

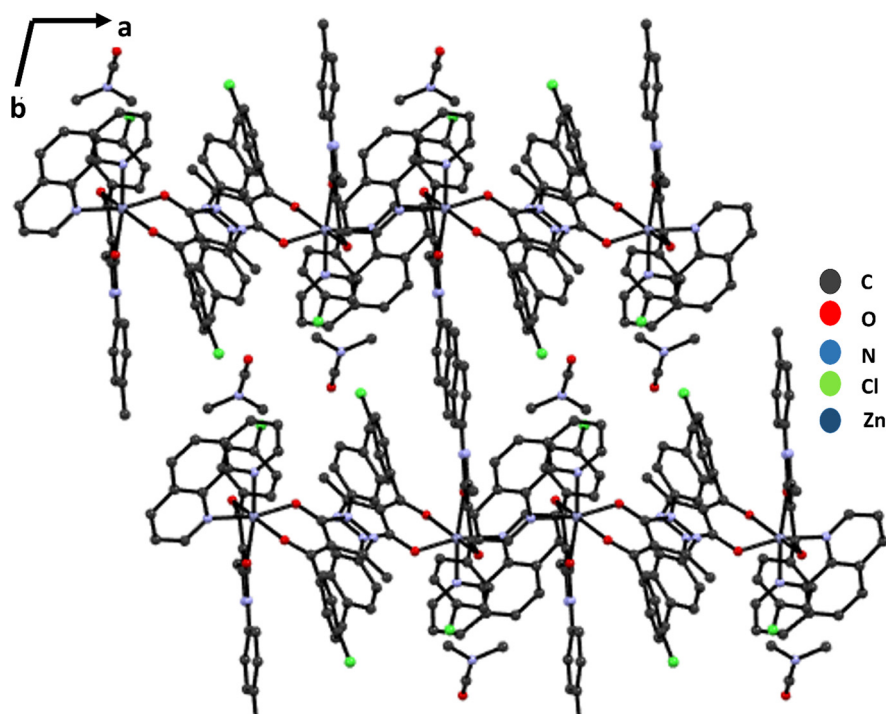


Fig. 8. Crystal packing system viewed down the 'c' axis of complex 3.

was due to loss of the lattice solvent molecule. A second degradation stage started after 250 °C due to pyrolysis of the primary (HL1) and secondary (bpy) ligands [4].

3.5.2. TGA of $[Zn(L2)_2(bpy)]$ (complex 2)

The TGA results revealed that the zinc complex 2 was air stable and it had high thermal stability (Fig. 10). Degradation observed

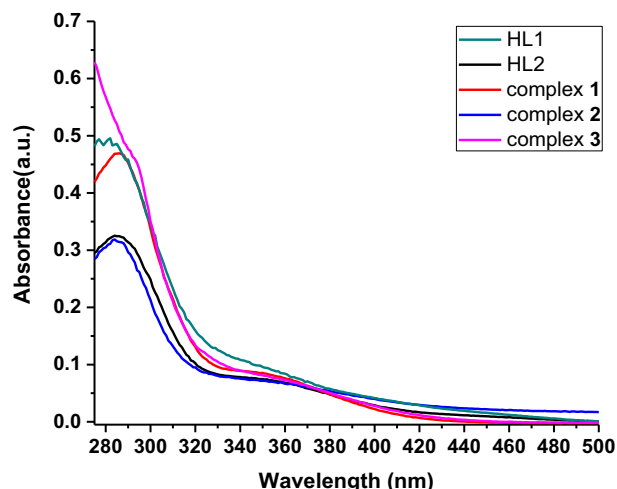


Fig. 9. UV-Vis spectra of the ligands and complexes 1–3.

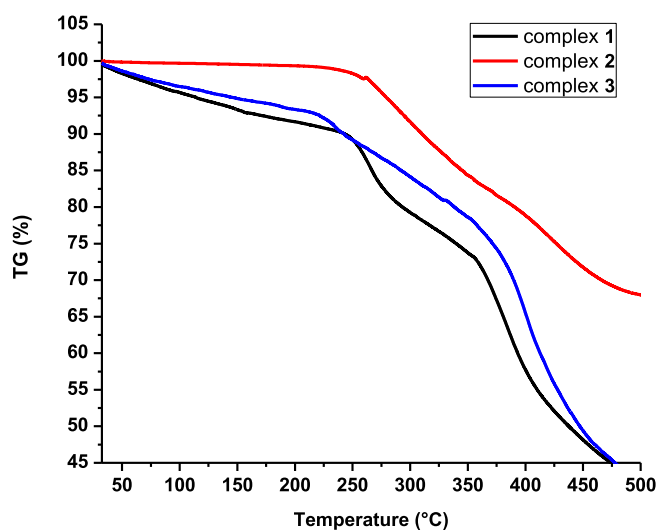


Fig. 10. TGA graphs of complexes 1–3.

after 240 °C was due to pyrolysis of the acyl pyrazolone (HL2) and secondary (bpy) ligands [4].

3.5.3. TGA of $[Zn(L2)_2(phen)]$ (complex 3)

Complex 3 was found to be air stable and to have high thermal stability from its TGA plot (Fig. 10). Degradation observed after 250 °C was due to pyrolysis of the ligand HL2 and the secondary ligand (phen) [4].

3.5.4. Antimalarial activity of the compounds

All five derivatives under study (the two ligands and three complexes) exhibited considerable inhibitory effects against *P. falciparum* in the *in-vitro* assay (Fig. 11). The lowest minimal inhibitory concentration of 0.11 $\mu\text{M/L}$ was obtained for complex 1, followed by 0.14, 0.95, 2.97 and 4.50 $\mu\text{M/L}$ respectively for complex 2, complex 3, HL2 and HL1.

4. Conclusion

Two acyl pyrazolones (HL1 and HL2) have been synthesized. A single crystal X-ray diffraction study revealed that the ligands HL1 and HL2 have inter-molecular and intra-molecular H-bonds, respectively. Three Zn(II) complexes (1–3) of these two ligands have been synthesized and characterized by various analytical and spectroscopic techniques. X-ray diffraction has confirmed their structures. The low molar conductance in DMSO indicated the non-electrolyte property of these complexes. Complexes 1–3 possess a distorted octahedral coordination geometry, with four coordination sites being occupied by two 4-acyl pyrazolone ligands and two coordination sites being occupied by the bidentate ligand (bpy or phen) (Fig. 1). The ligands and complexes have been screened for antimalarial activity. Complex 1 is reported to have the best activity from an *in vitro* *P. falciparum* growth inhibition assay. The present study reveals the possibility of complex 1 being a candidate for an antimalarial drug.

CRedit authorship contribution statement

Irfan Shaikh: Methodology, Software, Data curation, Writing - original draft, Investigation. **R.N. Jadeja:** Conceptualization, Supervision, Writing - review & editing. **Rajesh Patel:** Software, Validation, Visualization.

Declaration of Competing Interest

The authors declare that they have no known competing financial interests or personal relationships that could have appeared to influence the work reported in this paper.

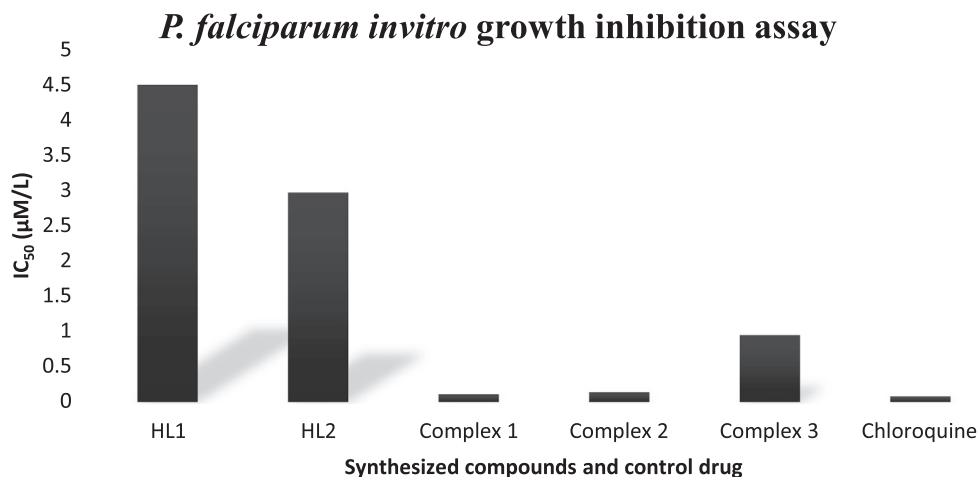


Fig. 11. Antimalarial activity of the synthesized compounds. *P. falciparum* was used in the *in vitro* assay.

Acknowledgements

The authors are thankful to the Head, Department of Chemistry for providing the necessary facilities required to carry out this work. The authors are also thankful to DST-PURSE for the NMR facility and DST-FIST for the single crystal X-ray diffraction instrument facilities in the Department of Chemistry.

Funding

This research did not receive any specific grant from funding agencies in the public, commercial or not-for-profit sectors.

Appendix A. Supplementary data

CCDC 1985004–1985008 contain the supplementary crystallographic data for complex **1**, complex **2**, complex **3**, HL1 and HL2 respectively. This data can be obtained free of charge at www.ccdc.cam.ac.uk/conts/retrieval.html or from the Cambridge Crystallographic Data Center, 12 Union Road, Cambridge CB2 1EZ, UK; fax: +44 1223/ 336 033. Email: deposit@ccdc.ac.uk. Supplementary data to this article can be found online at <https://doi.org/10.1016/j.poly.2020.114528>.

References

- [1] F. Marchetti, J. Palmucci, C. Pettinari, R. Pettinari, S. Scuri, I. Grappasonni, M. Cocchioni, M. Amati, F. Lejj, A. Crispini, *Inorg. Chem.* 55 (2016) 5453–5466.
- [2] F. Marchetti, C. Pettinari, R. Pettinari, *Coord. Chem. Rev.* 249 (2005) 2909–2945.
- [3] I. Shaikh, A. Vohra, R. Devkar, R. Jadeja, *Eur. J. Chem.* 10 (2) (2019) 131–138.
- [4] I.U. Shaikh, R.K. Patel, V.A. Mevada, V.K. Gupta, R.N. Jadeja, *ChemistrySelect* 4 (2019) 8286–8294.
- [5] K.M. Vyas, R.N. Jadeja, V.K. Gupta, K.R. Surati, *J. Mol. Struct.* 990 (2011) 110–120.
- [6] R.N. Jadeja, M. Chhatrola, V.K. Gupta, *Polyhedron* 63 (2013) 117–126.
- [7] R.N. Jadeja, K.M. Vyas, V.K. Gupta, R.G. Joshi, C. Ratna Prabha, *Polyhedron* 31 (2012) 767–778.
- [8] R.J. Yadav, K.M. Vyas, R.N. Jadeja, *J. Coord. Chem.* 63 (2010) 1820–1831.
- [9] M.C. Thounaojam, R.N. Jadeja, M. Valodkar, P.S. Nagar, R.V. Devkar, S. Thakore, *Food Chem. Toxicol.* 49 (2011) 2990–2996.
- [10] K.M. Vyas, R.N. Jadeja, D. Patel, R.V. Devkar, V.K. Gupta, *Polyhedron* 80 (2014) 20–33.
- [11] K. Nakum, R.N. Jadeja, *Z. Naturforsch B* 73 (2018) 713–718.
- [12] S.J. Archibald, 6.8 - Zinc, in J.A. McCleverty, T.J.B.T.-C.C.C.I.I. Meyer (Eds.), Pergamon, Oxford, 2003: pp. 1147–1251.
- [13] E.C. Fusch, B. Lippert, *J. Am. Chem. Soc.* 116 (1994) 7204–7209.
- [14] C.C. Hardin, A.G. Perry, K. White, *Biopolymers* 56 (2001) 147–194.
- [15] R. Carter, K.N. Mendis, *Clin. Microbiol. Rev.* 15 (2002) 564–594.
- [16] H. Caraballo, K. King, H. Caraball, *Emerg. Med. Pract.* 16 (2014) 1–4.
- [17] G. Kumar, O. Tanwar, J. Kumar, M. Akhter, S. Sharma, C.R. Pillai, M.M. Alam, M. S. Zama, *Eur. J. Med. Chem.* 149 (2018) 139–147.
- [18] J. Wang, G.-C. Xu, Y.-P. Zhang, H.-Y. Luo, J.-Y. Li, L. Zhang, D.-Z. Jia, *New J. Chem.* 43 (2019) 2529–2539.
- [19] J. Quirante, D. Ruiz, A. Gonzalez, C. Lopez, M. Cascante, R. Cortes, R. Messegueur, C. Calvis, L. Baldoma, A. Pascual, Y. Guerardel, B. Pradines, M. Font-Bardia, T. Calvet, C. Biot, *J. Inorg. Biochem.* 105 (2011) 1720–1728.
- [20] C. Hemmert, A. Fabie, A. Fabre, F. Benoit-Vical, H. Gornitzka, *Eur. J. Med. Chem.* 60 (2013) 64–75.
- [21] S. Pandey, P. Agarwal, K. Srivastava, S. Rajakumar, S.K. Puri, P. Verma, J.K. Saxena, A. Sharma, J. Lal, P.M.S. Chauhan, *Eur. J. Med. Chem.* 66 (2013) 69–81.
- [22] N.B. de Souza, A.M.L. Carmo, D.C. Lagatta, M.J.M. Alves, A.P.S. Fontes, E.S. Coimbra, A.D. da Silva, C. Abramo, *Biomed. Pharmacother.* 65 (2011) 313–316.
- [23] University of Göttingen, G.M. Sheldrick, SHELXS97 and SHELXL97, Germany, 1997.
- [24] C.K. Johnson, ORTEP II; Report ORNL-5138, Oak Ridge, TN, 1976.
- [25] A.L. Spek, PLATON for Windows, September, University of Utrecht, Netherlands, 1999.
- [26] M. Nardelli, *J. Appl. Crystallogr.* 28 (1995) 659–665.
- [27] K.H. Rieckmann, G.H. Campbell, L.J. Sax, J.E. Mrema, *Lancet* (London, England). 1 (1978) 22–23.
- [28] C. Lambros, J.P. Vanderberg, *J. Parasitol.* 65 (1979) 418–420.
- [29] J. Singh, *Indian J. Malariol.* 10 (1956) 117–129.
- [30] B. Kumar, K.J. Nakum, R.N. Jadeja, R. Kant, V.K. Gupta, *Acta Crystallogr. Sect. E* 71 (2015) 280–281.
- [31] H. Li, G.-C. Xu, L. Zhang, J.-X. Guo, D.-Z. Jia, *Polyhedron* 55 (2013) 209–215.
- [32] Z.-Y. Yang, R.-D. Yang, F.-S. Li, K.-B. Yu, *Polyhedron* 19 (2000) 2599–2604.
- [33] H.-Y. Luo, J.-Y. Li, Y. Li, L. Zhang, J.-Y. Li, D.-Z. Jia, G.-C. Xu, *RSC Adv.* 6 (2016) 114997–115009.